

Line shape of coherent population trapping resonance in the Λ -scheme under Ramsey-type interrogation in an optically dense medium

K.A. Barantsev, E.N. Popov, A.N. Litvinov

Abstract. We report a study of the Ramsey technique for detecting coherent population trapping resonance in a cold rarified ensemble of atoms with the collective effects related to its finite optical thickness taken into account. It is found that with the growth of the optical thickness of the medium the Ramsey comb becomes shifted with its maxima ‘trimmed’. The possibility of producing a region of maximal atomic excitation near the exit from the medium is found.

Keywords: coherent population trapping resonance, Λ -scheme, Ramsey detection technique.

1. Introduction

The interaction of bichromatic radiation with a three-level quantum system is known to give rise to the so-called dark state, when the radiation no more interacts with the quantum system. Experimentally this state manifests itself as the appearance of a transparency window. The presence of this feature is referred to as the effect of coherent population trapping (CPT) [1–4]. Under pulsed irradiation, or in the case of an optically dense medium, or when the Rabi frequencies of the radiation components are different, it is more common to speak of the related effect of electromagnetically induced transparency (EIT) [5,6]. Under the CPT or EIT conditions, the transparency window width can be considerably below the natural linewidth of an optical transition, amounting to hundreds (or even tens) of hertz [7–12]. This fact allows these effects to be used in multiple practical applications, including quantum frequency standards [13–18], optical magnetometers [19–23], inversionless laser oscillation [24,25], ultrahigh resolution spectroscopy [26], optical communications [27–29], facilities for recording and processing quantum information [30–33], and laser cooling of atoms [34–37].

The CPT phenomenon has been investigated for more than 40 years. During this time, a wide scope of problems has been studied related both to different conditions of the CPT observation and to different factors affecting the shape of CPT resonances. The performance improvement in metrological devices is achieved due to an increase in the contrast of the reference resonance, i.e. the ratio of the resonance ampli-

tude to its width, and reducing the light-induced shifts. One of the major lines of CPT investigations is the search for the ways to reduce the resonance linewidth. Essential narrowing of the CPT resonance line can be achieved by implementing the so-called Ramsey narrowing scheme [38]. First, it is possible by using the traditional free flight scheme. Thus, in Ref. [39] the parameters of CPT were studied in the case of exciting spatially separated regions of the bichromatic field. Second, one can use zone pumping that leads to an analogue of the Ramsey scheme [40]. In this geometry of CPT excitation, the diffusion of alkali atoms in the direction perpendicular to the laser beam leads to the limited time of interaction between the atom and the field. This fact makes it possible to observe the ‘Ramsey’ narrowing of the CPT resonance in cells both with a buffer gas, and with an anti-relaxation wall coating [41–42].

The third version of CPT resonance line narrowing is the pulsed pumping, i.e., the ‘temporal’ Ramsey scheme. Recently, extensive studies have been conducted in this field. Thus, the use of pulsed pumping allowed the authors of Ref. [43] to demonstrate the possibility of increasing the resolution and of separating a few peaks from the CPT resonance. The study of excitation of dark resonances by polychromatic radiation in cells with a buffer gas was analysed in Ref. [44]. In Ref. [45] the Ramsey multizone pumping of the CPT resonance was studied and an increased resolution power of the CPT signal was demonstrated. The application of pulsed pumping as a way of essential reduction of light-induced shifts was studied in Refs [46,47]. The narrowing of the CPT resonance can be also observed under the synchronised modulation of the polarisation of laser radiation [48]. A series of papers is devoted to the double-stage pulsed pumping. We would like to mention Ref. [49], where a synthetic frequency protocol for Ramsey spectroscopy is proposed that allows suppression of light-induced shifts. This pumping technique also allows an increase in the signal-to-noise ratio [50]. The possibility of controlling the decay of the excited levels in the presence of pulsed fields is considered in Ref. [51]. The authors of Ref. [52] consider the role of incoherent scattering channel in the propagation of pulsed radiation under the EIT conditions in optically dense media.

Besides the small linewidth of the CPT resonance, its amplitude is also of importance. The main way to increase it is to use greater concentrations of atoms. At the initial stage of increasing the concentration of atoms, the amplitude grows proportionally to their number. After achieving a certain concentration, the collective effects begin to manifest themselves, and the dependence of the amplitude on the concentration of atoms becomes nonlinear. The study of collective effects in

K.A. Barantsev, E.N. Popov, A.N. Litvinov Peter the Great St. Petersburg Polytechnic University, ul. Politekhnikeskaya 29, 195251 St. Petersburg, Russia; e-mail: kostmann@yadex.ru, andrey.litvinov@mail.ru

Received 5 March 2018; revision received 3 May 2018
Kvantovaya Elektronika 48 (7) 615–620 (2018)
Translated by V.L. Derbov

rarified media has shown that in this case the interference phenomena can take place [53, 54]. From a series of papers on CPT in optically dense media, it is known that the presence of absorption in the medium can lead to the spectrum distortion and, therefore, to a change in CPT resonance shape [55], to increased correlation between the laser radiation modes when using partially correlated laser fields [56], and to appearance of polarisation ellipticity in the case of pumping alkali atoms [57]. Collective effects in rarified media can also lead to single-photon superradiation that appears under the pulsed excitation of ensembles of cold atoms [58, 59]. Thus, a question arises how the collective effects will manifest themselves in optically dense rarified media under the conditions of CPT with pulsed pumping (Ramsey detection scheme). The present paper is devoted to this issue.

2. Formulation of the problem

Consider an ensemble of cold atoms at the temperature that allows the Doppler and collisional broadening of the absorption line to be neglected. The atoms possess three energy levels, two lower ones, $|1\rangle$ and $|2\rangle$, of the ground state and the upper energy level $|3\rangle$ of the excited state (Fig. 1a). The transitions $|1\rangle \rightarrow |3\rangle$ and $|2\rangle \rightarrow |3\rangle$ lie in the optical region, and the transition $|1\rangle \rightarrow |2\rangle$ in the microwave range. The ensemble has a prolate cigar-like shape and is optically dense along the z axis (Fig. 1b), i.e., the mean free path of a quasi-resonance photon in this direction is much smaller than the length of the ensemble L : $n_a \lambda^2 L \gg 1$, where n_a is the concentration of atoms, and λ is the resonance wavelength. In the transverse direction the ensemble is optically thin, which allows the scattered light and the interference effects related to it to be neglected, since the photons scattered aside leave the ensemble with great probability. Below we consider the situation when the ensemble of atoms is sufficiently rarified, i.e., on an average, less than one atom fall on a resonance wavelength: $n_a \lambda^3 < 1$. This fact makes it possible to neglect the resonance dipole–dipole interaction of atoms in the near-field zone and the effects of recurrent light scattering [60–62]. However, the fields created by the atoms in the wave zone, are added, and the signal at the detector is a superposition of the incident laser radiation and the fields of atoms of the ensemble. Thus,

in the present problem it is necessary to take the collective effects in rarified media into account.

The essence of the Ramsey detection technique consists in acting with two pulses of radiation on the ensemble on atoms. The pulses have the carrier frequencies ν_1 and ν_2 , close to the resonance with the transitions $|1\rangle \rightarrow |3\rangle$ and $|2\rangle \rightarrow |3\rangle$, respectively. In the approximation of a plane wave front, the electric field of the pulses propagating along the z axis has the form:

$$E(z, t) = E_1^0(z, t) \exp[-i(\nu_1 t - k_1 z)] + E_2^0(z, t) \exp[-i(\nu_2 t - k_2 z)] + \text{c.c.}, \quad (1)$$

where $E_j^0(z, t)$; $j = 1, 2$ are the complex amplitudes; and k_j are the wavenumbers. Thus, the Λ -scheme of interaction is obtained (Fig. 1a).

The first laser pulse induces low-frequency coherence in the atoms and transfers them into the state of coherent population trapping. Its duration τ_p should be greater than the minimal time of the CPT state stabilisation. This is determined by the inequality $\tau_p > \gamma/\Omega^2$, where γ is the decay rate of the excited state $|3\rangle$; and Ω is the characteristic Rabi frequency.

After the passage of the first pulse, a dark pause with the duration T begins. During the pause the population of the excited energy level $|3\rangle$ and the optical coherences of atoms are destroyed due to the spontaneous decay; however, the low-frequency coherence has much greater lifetime (by a few orders of magnitude) and does not decay until the second pulse comes. During this time the free evolution of the low-frequency coherence occurs. If the two-photon detuning of radiation from the transition $|1\rangle \rightarrow |2\rangle$ is δ , then the low-frequency coherence acquires the phase shift δT with respect to the radiation phase.

The second pulse serves to detect this phase shift. The duration of the second pulse should be smaller than the time of the CPT state stabilisation: $\tau \ll \gamma/\Omega^2$. Depending on the phase shift, the action of the second pulse leads to different consequences. If the phase shift is $2\pi n$ ($n = 0, 1, 2, \dots$), then the second pulse comes in phase with the low-frequency coherence and does not destroy it. The atoms stay in the CPT state and do not scatter light, so that the pulse weakly changes after passing through the medium, and the detector records a transmission peak. Otherwise, the second pulse destroys the low-frequency coherence, which leads to considerable absorption of the pulse.

3. Mathematical model

The state of the atomic ensemble affected by the above pulses can be described by the equation for the single-particle density matrix. Since the ensemble is kept at a low temperature (such that one can neglect Doppler broadening and collisions), it is valid to consider the atoms as quasi-immobile. Moreover, in the approximation of a plane front of the wave propagating along the z axis the problem can be made one-dimensional. After these simplifications, the density matrix equation takes the form

$$\frac{\partial}{\partial t} \rho_{kj}(z, t) = -i[\hat{V}, \hat{\rho}(z, t)]_{kj} + i\omega_{jk} \rho_{kj}(z, t) + R, \quad (2)$$

where R describes the spontaneous emission; and ω_{jk} is the frequency of the appropriate atomic transition.

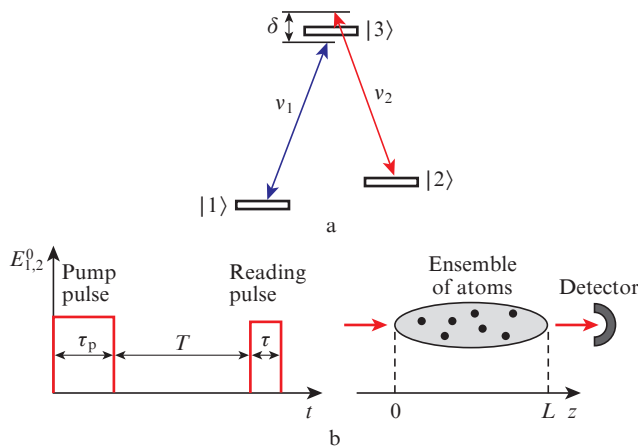


Figure 1. (a) Energy level diagram of atoms interacting with the double-frequency laser radiation and (b) shape of laser pulses and geometry of the problem.

The interaction operator \hat{V} is written in the dipole approximation as

$$\hbar \hat{V} = -\hat{\mathbf{d}}\mathbf{E}, \quad (3)$$

where the laser field \mathbf{E} is given by Eqn (1); and $\hat{\mathbf{d}}$ is the atomic dipole moment operator.

Let us assume that the polarisation of the incident wave is collinear with the dipole moment vector for the considered transition, i.e., $\hat{\mathbf{d}}\mathbf{E} = \hat{d}E$. In the rotating-wave approximation, the interaction operator takes the form:

$$\begin{aligned} \hbar \hat{V} = & -d_{31}E_1^0(z, t) \exp[-i(v_1 t - k_1 z)] |3\rangle\langle 1| \\ & - d_{32}E_2^0(z, t) \exp[-i(v_2 t - k_2 z)] |3\rangle\langle 2| + \text{H.c.}, \end{aligned} \quad (4)$$

where d_{jk} are the matrix elements of the dipole moment operator.

Substituting the interaction operator (4) into Eqn (2) and extracting the fast-oscillating factor $\rho_{ik} = \tilde{\rho}_{ik} \exp(iv_j t)$, $\tilde{\rho}_{ii} = \rho_{ii}$ from the nondiagonal elements of the density matrix (atomic coherences), we arrive at the system of differential equations that describe the dynamics of the density matrix of atoms at the position z :

$$\begin{aligned} \dot{\rho}_{11} = & \Gamma_{||}(\rho_{22} - \rho_{11}) + \gamma_{13}\rho_{33} + i\Omega_1^* \tilde{\rho}_{13} - i\Omega_1 \tilde{\rho}_{31}, \\ \dot{\rho}_{22} = & \Gamma_{||}(\rho_{11} - \rho_{22}) + \gamma_{23}\rho_{33} + i\Omega_2^* \tilde{\rho}_{23} - i\Omega_2 \tilde{\rho}_{32}, \\ \dot{\rho}_{33} = & -(\gamma_{13} + \gamma_{23})\rho_{33} - i\Omega_1^* \tilde{\rho}_{13} + i\Omega_1 \tilde{\rho}_{31} - i\Omega_2^* \tilde{\rho}_{23} + i\Omega_2 \tilde{\rho}_{32}, \\ \dot{\tilde{\rho}}_{12} = & [-i(\Delta_1 - \Delta_2) - \Gamma_{\perp}] \tilde{\rho}_{12} + i\Omega_2^* \tilde{\rho}_{13} - i\Omega_1 \tilde{\rho}_{32}, \\ \dot{\tilde{\rho}}_{13} = & (-i\Delta_1 - \gamma_{13}/2) \tilde{\rho}_{13} + i\Omega_1(\rho_{11} - \rho_{33}) + i\Omega_2 \tilde{\rho}_{12}, \\ \dot{\tilde{\rho}}_{23} = & (-i\Delta_2 - \gamma_{23}/2) \tilde{\rho}_{23} + i\Omega_2(\rho_{22} - \rho_{33}) + i\Omega_1 \tilde{\rho}_{21}. \end{aligned} \quad (5)$$

Here $\gamma = \gamma_{13} + \gamma_{23}$ is the total spontaneous decay rate of the energy level $|3\rangle$; $\gamma_{13} \approx \gamma_{23} \approx \gamma/2$ is the decay rate of the energy level $|3\rangle$ via the appropriate optical transition; $\Gamma_{||}$ is the rate of population mixing between the levels $|1\rangle$ and $|2\rangle$; Γ_{\perp} is the decay rate of the low-frequency coherence; $\Delta_j = v_j - \omega_{3j}$ are the detunings of the fields; $j = 1, 2$; and $\Omega_j = -d_{3j}E_j^0/\hbar$ are the Rabi frequencies.

The propagation of radiation through the medium is described by reduced wave equations for complex amplitudes of the fields. The right-hand side describes the response of the medium determined by its polarisation $P_j(z, t)$:

$$\frac{\partial E_j^0(z, t)}{\partial z} + \frac{1}{c} \frac{\partial E_j^0(z, t)}{\partial t} = 4\pi i P_j^0(z, t) k_j, \quad (6)$$

where $P_j^0(z, t)$ is the slow-varying amplitude of polarisation, oscillating with optical frequency; and c is the velocity of light in vacuum.

The polarisation of the medium can be found from the density matrix of the atomic subsystem as the quantum mechanical average of the dipole moment density:

$$P(z, t) = n_a \text{Sp}(\hat{\rho}(z, t) \hat{\mathbf{d}}). \quad (7)$$

Substituting Eqn (7) into Eqn (6) and rewriting the equations in terms of Rabi frequencies, we obtain

$$\frac{\partial \Omega_j(z, t)}{\partial z} + \frac{1}{c} \frac{\partial \Omega_j(z, t)}{\partial t} = \frac{4\pi i n_a |d_{j3}|^2 v_j}{c\hbar} \tilde{\rho}_{3j}(z, t). \quad (8)$$

Simultaneous solution of Eqns (5) for the atomic density matrix and Eqns (8) for the field propagation yields the information about the dynamics of populations and coherences in the atomic ensemble and on the field distribution along the z axis.

4. Basic results and discussion

Figure 2 presents the modification of the detecting pulse shape after its transmission through the ensemble of atoms. In the case $\delta T = \pi$ [curve (3)] the output pulse is considerably absorbed as compared to the input pulse [curve (1)]; one can see transient processes at the beginning and at the end of the pulse. The characteristic time of these processes is determined by the lifetime of the excited state γ^{-1} , so that the lower bound for the detecting pulse duration is $\tau > \gamma^{-1}$. In the case $\delta T = 2\pi$ [curve (2)], the pulse absorption is weak, i.e., the Ramsey resonance takes place.

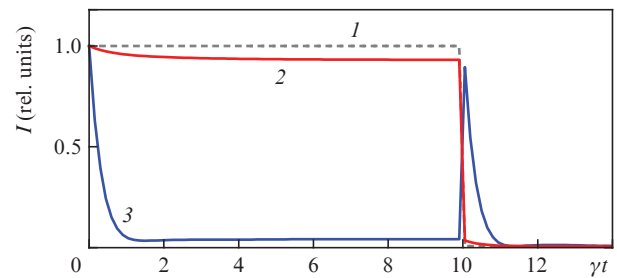


Figure 2. Shape of the detecting pulse at the input (1) and output [(2), $\delta T = \pi$ and (3), $\delta T = 2\pi$] of the atomic ensemble. The output pulses are given for two values of the two-photon detuning, corresponding to the maximum and minimum of absorption. The reading pulse duration, $\tau = 10\gamma^{-1}$; the dark pause, $T = 8$ ms; the Rabi frequencies at the pulse maximum, $\Omega_1 = \Omega_2 = 0.01\gamma$; the concentration of atoms, $n_a = 5 \times 10^{10} \text{ cm}^{-3}$; the medium length, $L = 200 \mu\text{m}$; the optical thickness, $n_a \lambda^2 L \sim 5$; and the spontaneous decay rate of the excited level, $\gamma = 10^7 \text{ s}^{-1}$.

The intensity of radiation at the detector $I(z = L, t)$ can be found from the system of equations (5)–(8):

$$I(z, t) \sim \langle E(z, t)^2 \rangle = |E_1^0(z, t)|^2 + |E_2^0(z, t)|^2, \quad (9)$$

where $E(z, t)$ is the electric field strength, expressed by Eqn (1); and $\langle \dots \rangle$ denotes averaging over the period of beats at the frequency of the transition $v_1 - v_2$. Thus, the cross terms in Eqn (9), oscillating with the difference frequency, are turned to zero. The beating period amounts to ~ 1 ns for the transition frequency $|1\rangle \rightarrow |2\rangle$ in the microwave range, which is much smaller than $\gamma^{-1} \sim 100$ ns. Therefore, the pulse shape in Fig. 2 is well resolved.

For the discrimination curve formation let us consider the energy W of the detecting pulse as a signal:

$$W = \int_0^\infty I(L, t) dt. \quad (10)$$

Certainly, in numerical computation, as well as in the experiment, the upper limit of this integral is replaced with a finite value after the total termination of the pulse. Figure 3a presents

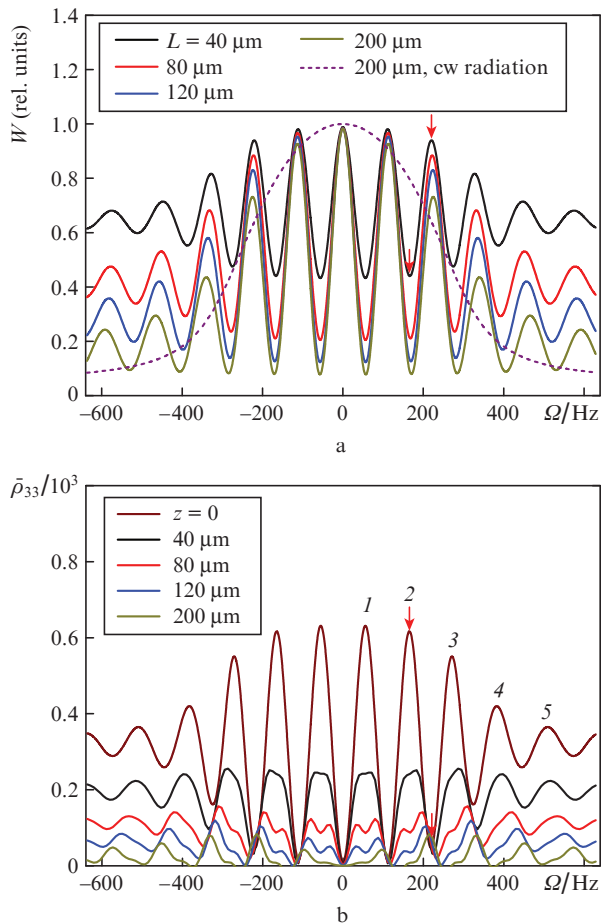


Figure 3. (Colour online) (a) Forward radiation signal for different lengths L of the atomic ensemble and (b) the population of the excited state for different values of the coordinate z . The arrows indicate two values of detuning, for which the dependences shown in Fig. 5 are plotted. The parameters are similar to those in Fig. 2.

the dependence of the detecting pulse energy W at the output from the atomic ensemble on the two-photon detuning. The curves representing the Ramsey comb are shown for different lengths L of the medium. For comparison, the shape of the cw-pumped CPT resonance is presented.

The contrast of the central peak increases with the medium length, since the formation of the signal requires a certain optical density. One can also see the shift of the side maxima position with the variation of L . The physical reason of this shift can be clarified by analysing the dependence of the excited state population ρ_{33} on the coordinate z .

Figure 3b presents the dependences of the population averaged over the time of the detecting pulse

$$\bar{\rho}_{33}(z) = \frac{1}{\tau} \int_0^{\tau} \rho_{33}(z, t) dt, \quad (11)$$

on the two-photon detuning for different values of the coordinate z . One can see that due to the absorption of radiation the Ramsey comb is modified, which looks as ‘trimming’ of the peaks. The peaks become asymmetric as strongly as the envelope (the CPT resonance pumped by cw radiation) is tilted with respect to the horizontal direction. Thus, peaks (1) and (5) in Fig. 3b preserve their symmetry under the

growth of z , while peaks (2) and (3) acquire asymmetry and shift, since their left-hand wing decreases stronger. Thus, the shift of the peaks is maximal in the region where the modulus of the envelope derivative achieves the maximal value.

The shifts of the maxima and minima of the Ramsey comb are presented in Fig. 4.

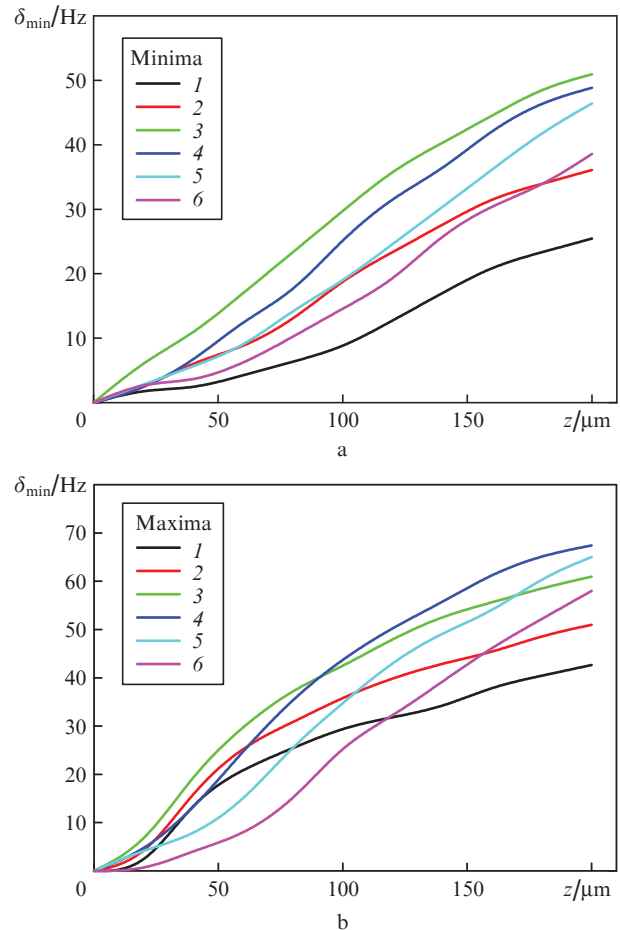


Figure 4. (Colour online) Shifts of (a) minima and (b) maxima of the Ramsey comb, presented in Fig. 3b, as functions of coordinate z .

Curve (3) for the position of the minimum (Fig. 4a) lies above the rest ones, since the maximum of the envelope derivative is achieved. For the positions of maxima the situation is similar, and the greatest shift occurs for maxima (3) and (4) (Fig. 4b).

Since the maximum for large z shifts, it can partially overlap a minimum for small z , which is seen indeed in Fig. 3b for the two-photon detuning $\delta = 215$ Hz (marked by a vertical arrow). Therefore, this value of the two-photon detuning exists, for which the dependence of the excited level population on the coordinate z demonstrates increasing behaviour (Fig. 5a). The intensity of atomic fluorescence is determined by the population of the excited level; therefore, the Ramsey resonance in Fig. 3b can be obtained by detecting the fluorescence of the atomic ensemble. Then, according to Fig. 5a, the deep layers of the medium will fluoresce stronger than the initial ones.

Let us choose the second value of the two-photon detuning, for which the population maximum is achieved at the medium

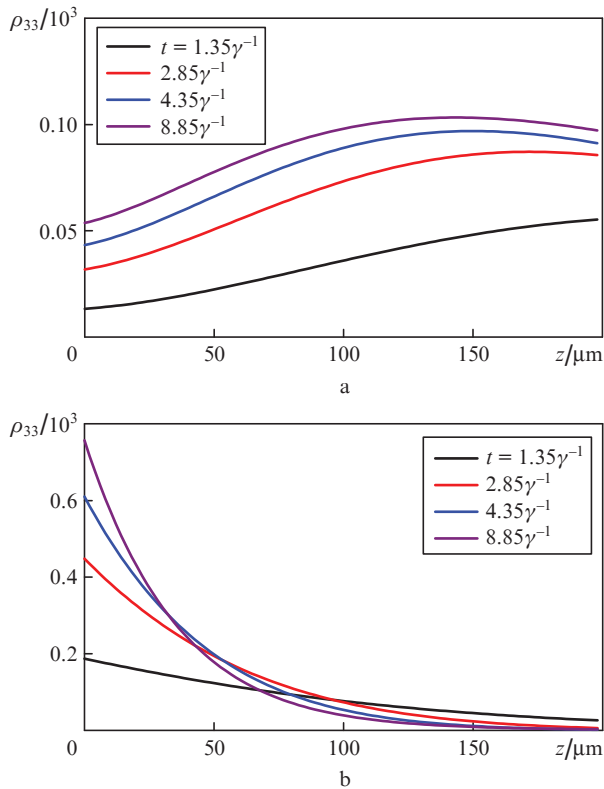


Figure 5. (Colour online) Population of the excited level as a function of the coordinate z at different moments of time during the reading pulse action for the detuning $\delta =$ (a) 215 and (b) 167 Hz. The parameters are similar to those used in Fig. 2.

input ($\delta = 167$ Hz, an arrow in Fig. 3b). The population decrease along the z axis for this value of detuning is shown in Fig. 5b.

The observed fall of population is due to the exponential decrease in the radiation intensity, since the detuning $\delta = 167$ Hz corresponds to the absence of the CPT state.

5. Conclusions

In the present paper we report the theory of coherent population trapping resonance, detected using the Ramsey method, under the conditions of finite optical thickness and the presence of collective effects in the rarified medium. The medium is a cloud of cold atoms, in which the mean interatomic distance exceeds the resonance wavelength, which allows the near-field interaction of atoms and the recurrent scattering of light to be neglected. The scheme of atomic energy levels is described by a three-level model, in which one level is excited, and two ground ones form a forbidden transition. The medium is exposed to bichromatic radiation that consists of two sequential pulses, implementing the Ramsey detection scheme. The carrier frequencies of the field are in resonance with the optical transitions of atoms and form a Λ -scheme of excitation. The mathematical model comprises the dynamic equation for the atomic density matrix, solved simultaneously with the wave equation for the electromagnetic field propagation and allowing for the collective effects, related to the superposition of the fields, created by the atoms in the wave zone.

The calculations of the detecting pulse energy and the excited level population averaged over the duration of the

pulse are presented. It was found that the Ramsey ‘comb’ is modified as the field passes through the medium, namely, the peaks are changed in amplitude and shifted. The maximal shift takes place for the two-photon detuning that provides a maximum of the Ramsey resonance envelope derivative.

It is found that in an optically dense medium one can create the distribution of atomic excitation having the greatest value at the end of the medium. The reason is that the detecting pulse passes the initial part of the medium being in the CPT state practically without absorption, and in the end part of the medium the position of the resonance shifts and the CPT conditions are no more valid. Hence, the pulse is absorbed and ensures atomic excitation.

Acknowledgements. The work was supported by the Russian Science Foundation (Project No. 17-12-01085). The authors are grateful to I.M. Sokolov for useful consultations.

References

1. Alzetta G. et al. *Nuovo Cim. B*, **36** (1), 5 (1976).
2. Arimondo E., Orriols G. *Lett. Nuovo Cim.*, **17** (10), 333 (1976).
3. Gray H.R., Whitley R.M., Stroud C.R. Jr. *Opt. Lett.*, **3**, 218 (1978).
4. Agap'ev B.D., Gornyi M.B., Matisov B.G., Rozhdestvenskii Yu.V. *Phys. Usp.*, **36** (9), 763 (1993) [*Usp. Fiz. Nauk*, **163** (9), 1 (1993)].
5. Gornyi M.B., Matisov B.G., Rozhdestvenskii Yu.V. *JETP*, **68** (4), 728 (1989) [*Zh. Eksp. Teor. Fiz.*, **95**, 1263 (1989)].
6. Arimondo E. *Progr. Optics*, **35**, 257 (1996).
7. Wynands R., Nagel A. *Appl. Phys. B*, **68**, 1 (1999).
8. Erhard M., Helm H. *Phys. Rev. A*, **63**, 043813 (2001).
9. Merimaa M., Lindvall Th., Tittonen I., Ikonen E. *J. Opt. Soc. Am. B*, **20**, 273 (2003).
10. Balabas M.V., Karaulanov T., Ledbetter M.P., Budker D. *Phys. Rev. Lett.*, **105**, 070801 (2010).
11. Datsyuk V.M., Sokolov I.M., Kupriyanov D.V., Havey M.D. *Phys. Rev. A*, **77**, 033823 (2008).
12. Brazhnikov D.V., Taihenahev A.V., Tumaikin A.M., Yudin V.I. *Laser Phys. Lett.*, **11**, 125702 (2014).
13. Vanier J. *Appl. Phys. B*, **81**, 421 (2005).
14. Zibrov S.A., Velichansky V.L., Zibrov A.S., Taichenachev A.V., Yudin V.I. *JETP Lett.*, **82** (8), 477 (2005) [*Pis'ma Zh. Eksp. Teor. Fiz.*, **82** (8), 534 (2005)].
15. Kazakov G., Matisov B., Mazets I., et al. *Phys. Rev. A*, **72**, 063408 (2005).
16. Zibrov S.A., Novikova I., Phillips D.F., et al. *Phys. Rev. A*, **81**, 013833 (2010).
17. Barantsev K.A., Popov E.N., Litvinov A.N., Petrov V.M. *Radiotekhnika*, **12**, 164 (2016).
18. Khripunov S., Radnatarov D., Kobtsev S. *Proc. SPIE*, **9378**, 93780A (2015).
19. Akulshin A., Celikov A., Velichansky V. *Opt. Commun.*, **84**, 139 (1991).
20. Stahler M., Wynands R., Knappe S., et al. *Opt. Lett.*, **27**, 1472 (2002).
21. Shwindt P.D.D. et al. *Appl. Phys. Lett.*, **85**, 6409 (2004).
22. Yashuk V.V., Granwehr J., Kimbal D.F., et al. *Phys. Rev. Lett.*, **93**, 160801 (2004).
23. Cox K. et al. *Phys. Rev. A*, **83**, 015801 (2011).
24. Kocharovskaya O., Khanin Ya.I. *JETP Lett.*, **48**, 630 (1988) [*Pis'ma Zh. Eksp. Teor. Fiz.*, **48**, 581 (1988)].
25. Harris S. *Phys. Rev. Lett.*, **62**, 1022 (1989).
26. Vanier J., Godone A., Levi F. *Phys. Rev. A*, **58**, 2345 (1998).
27. Hau L.V. et al. *Nature*, **397**, 594 (1999).
28. Akulshin A.M., Cimmino A., Sidorov A.I., Hannaford P., Opat G.I. *Phys. Rev. A*, **67**, 011801(R) (2003).
29. Mikhailov E.E., Sautenkov V.A., Novikova I., Welh G.R. *Phys. Rev. A*, **69**, 063808 (2004).
30. Fleishhauer M., Lukin M.D. *Phys. Rev. Lett.*, **84**, 5094 (2000).
31. Liu C., Dutton Z., Behroozi C.H., Hau L.V. *Nature (London)*, **409**, 490 (2001).

32. Lukin M.D. *Rev. Modern Phys.*, **75**, 457 (2003).
33. Fleischhauer M., Imamoglu A., Marangos J.P. *Rev. Modern Phys.*, **77**, 633 (2005).
34. Aspet A., Arimondo E., Kaiser R., Vansteenkiste N., Cohen-Tannoudji C. *Phys. Rev. Lett.*, **61**, 826 (1988).
35. Kasevih M., Chu S. *Phys. Rev. Lett.*, **69**, 1741 (1992).
36. Mazets I.E., Matisov B.G. *JETP Lett.*, **60** (10), 703 (1994) [*Pis'ma Zh. Eksp. Teor. Fiz.*, **60**, 686 (1994)].
37. Taichenachev A.V., Tumaikin A.M., Yudin V.I. *JETP Lett.*, **65** (10), 779 (1997) [*Pis'ma Zh. Eksp. Teor. Fiz.*, **65**, 744 (1997)].
38. Ramsey N.F. *Nobel Lecture: Experiments with Separated Oscillatory Fields and Hydrogen Masers*. Nobelprize.org. Nobel Media AB 2014. Web. 30 Jun 2018. http://www.nobelprize.org/nobel_prizes/physics/laureates/1989/ramsey-lecture.html [*Usp. Fiz. Nauk*, **160** (12), 91 (1990)].
39. Sokolov I.M. *Quantum Electron.*, **45**, 947 (2015) [*Kvantovaya Elektron.*, **45**, 947 (2015)].
40. Xiao Y., Novikova I., Phillips D.F., Walsworth R.L. *Phys. Rev. Lett.*, **96**, 043601 (2006).
41. Breschi E., Kazakov G., Schori C., et al. *Phys. Rev. A*, **82**, 063810 (2010).
42. Kazakov G.A., Litvinov A.N., Matisov B.G., et al. *J. Phys. B*, **44**, 235401 (2011).
43. Grujić Z.D., Mijailović M., Arsenović D., Kovačević A., Nikolić M., Jelenković B.M. *Phys. Rev. A*, **78**, 063816 (2008).
44. Litvinov A., Kazakov G., Matisov B., et al. *J. Phys. B: At. Mol. Opt. Phys.*, **43**, 1 (2010).
45. Failache H., Lenci L., Lezama A. *Phys. Rev. A*, **81**, 023801 (2010).
46. Yano Y., Gao W., Goka S., Kajita M. *Phys. Rev. A*, **90**, 013826 (2014).
47. Pati G.S., Warren Z., Yu N., Shahriar M.S. *J. Opt. Soc. Am. B*, **32**, 388 (2015).
48. Yun P., Tricot F., Calosso C.E., Micalizio S., François B., Boudot R., Guérandel S., de Clercq E. *Phys. Rev. Appl.*, **7**, 014018 (2017).
49. Yudin V.I., Taichenachev A.V., Basalaev M.Yu. *Phys. Rev. A*, **93**, 013820 (2016).
50. Yano Y., Goka S., Kajita M. *Appl. Phys. B*, **123**, 67 (2017).
51. Nicolas L., Delord T., Jamonneau P., Coto R., Maze J., Jacques V., Hétet G. arXiv:1712.04240v1 [quant-ph].
52. Datsyuk V.M., Sokolov I.M., Kupriyanov D.V., Havey M.D. *Phys. Rev. A*, **74**, 043812 (2006).
53. Sokolov I.M., Kupriyanov D.V., Havey M.D. *Opt. Commun.*, **243**, 165 (2004).
54. Kupriyanov D.V., Sokolov I.M., Larionov N.V., et al. *Phys. Rev. A*, **69**, 033801 (2004).
55. Barantsev K.A., Popov E.N., Litvinov A.N. *JETP*, **121** (5), 758 (2015) [*Zh. Eksp. Teor. Fiz.*, **148**, 869 (2015)].
56. Barantsev K.A., Litvinov A.N., Popov E.N., *JETP*, **125** (6), 993 (2015) [*Zh. Eksp. Teor. Fiz.*, **152**, 1165 (2017)].
57. Barantsev K.A., Popov E.N., Litvinov A.N. *Quantum Electron.*, **47**, 812 (2017) [*Kvantovaya Elektron.*, **47**, 812 (2017)].
58. Scully M.O., Fry E.S., Ooi C.H.R., Wódkiewicz K. *Phys. Rev. Lett.*, **96**, 010501 (2006).
59. Kuraptsev A.S., Sokolov I.M., Havey M.D. *Phys. Rev. A*, **96**, 023830 (2017).
60. Kuraptsev A.S., Sokolov I.M. *Phys. Rev. A*, **90**, 012511 (2014).
61. Roof S., Kemp K., Havey M.D., Sokolov I.M., Kupriyanov D.V. *Opt. Lett.*, **40**, 1137 (2015).
62. Fofanov Ya.A., Kuraptsev A.S., Sokolov I.M., Havey M.D. *Phys. Rev. A*, **84**, 053811 (2011).